18th International Conference on Renewable Energies and Power Quality (ICREPQ'20)
Granada (Spain), 1st to 2nd April 2020
Renewable Energy and Power Quality Journal (RE&PQJ)
ISSN 2172-038 X, Volume No.18, June 2020

Comparative Analysis of Dynamic Performance Between Switched Reluctance Motors 6x4 and 8x6

M.B.S.Pinto, G.P.Viajante, E.N. Chaves, M.A.A. Freitas, M.E. Oliveira and J.A. Santos.

Federal Institute of Education, Science and Technology of Goiás
Energy Systems Research Center (Núcleo de Pesquisas em Sistemas de Energia - NuPSE)
Campus of Itumbiara – Goiás, (Brazil)
Phone/Fax number:+55 62996960086, e-mail: ghuterp@gmail.com and mathheusbueno@gmail.com

Abstract. This paper presents a comparative study between the Switched Reluctance Machine (SRM) 8x6 and 6x4 operating as a motor with both 60kW of power. The computer simulation was performed in Matlab™ / Simulink® environment and allowed the machine behavior under various operating conditions to be verified. This work made it possible to evaluate: phase voltage and current, speed, torque and efficiency. Comparative results between the two machines will be presented and discussed.

Key words. Electric vehicles, Energy efficiency, Switched Reluctance Motor 6x4, Switched Reluctance Motor 8x6.

1. Introduction

The growing demand for electricity from the lifestyle of modern society has made it necessary for more than one energy source to be studied and applied, taking into account the environmental and social impacts to be generated in the short and long term. As a result, the search for renewable energies has been rapidly expanding around the world such as solar, wind, biomass, geothermal and others[1]. In this context, several researches have been conducted in search of other alternatives such as the use of Switched Reluctance Motors in electric vehicles instead of the combustion motor.

In the last two decades, SRM have been on the rise due to their characteristics such as their structural simplicity, their robustness, phase-free tolerance, simplicity of control, low manufacturing cost, high temperature tolerance among others[2].

SRM construction is robust and inexpensive, assembled from a rotor and a stator, with protruding poles, non-oriented grain steel rolling and coils concentrated only on the stator poles. Its inductance is maximum when the rotor poles in relation to the stator are aligned and minimum when they are misaligned[3][4].

Due to its constructive characteristics, SRM has been increasingly explored in the area of electric traction. Several studies already perform their approach with the applications of electric traction, aiming to explore their particularities optimizing the machine according to the proposed application[5].

The machine is already being used in electric cars, city buses, trucks, backhoe loaders, railway locomotives, electric trams, battery vehicles, and more [6][7][8][9]. Thus reducing emissions of polluting gases such as CO_2 that is harmful to human life by contributing to the greenhouse effect, which raises the temperature of the earth.

2. Switched Reluctance Machine

The SRM has a double overhang structure with rotor excitation using phase separated windings. Each phase of the machine contains its windings gathered only on the stator projections, while the rotor is composed only of ferromagnetic material, thus not containing coils or magnets [10]. Fig. 1 represents the structure of a 6x4 and 8x6 SRM.

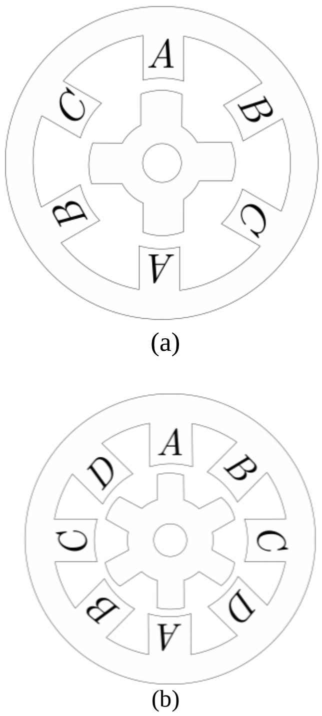

Fig.1. SRM 6x4 (a) and 8x6 (b) building structure.

In order to compare the two machines in question, the same parameters were considered. Table I shows the data of SRM 6x4 and 8x6 machines used in the present paper.

Table I. – Parameters of SRM 6x4 and 8x6.

Parameters	Values
Number of poles (stator and rotor)	8x6 e 6x4
Phase number	4 e 3
Output power	60KW
Stator resistance	0,05Ω
Moment of inertia	0,05 Kgm²
Alignment inductance	23,6mH
Misalignment inductance	0,67mH

The reluctance of the SRM magnetic circuit is dependent on the rotor position relative to the stator. In the aligned position, when a pair of rotor poles are aligned with a pair of stator poles, the magnetic circuit has minimal reluctance and therefore maximum inductance. Fig.2 shows the characteristic inductance curves of the machine.

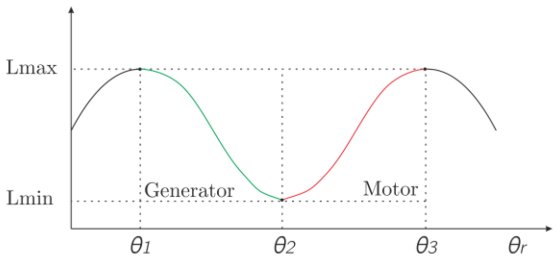

Fig.2. Inductance profile for an SRM.

3. Mathematical Model

For the development of the mathematical model was considered the two SRM operating as a motor. Fig.3 shows the equivalent phase circuit of the machine.

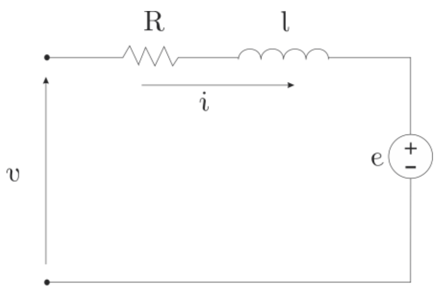

Fig.3. Equivalent circuit for one phase.

Initially, we can consider the voltage $(\boldsymbol{v})$ of the SRM terminals as:

$$\boldsymbol{v = Ri + \frac{d\varphi}{dt}} \qquad (1)$$

where φ corresponds to the magnetic flux of the stator coils and R the stator winding resistance, $\boldsymbol{i}$ is the phase current.

We can define the magnetic flux as:

$$\boldsymbol{\varphi(i,\theta) = l(i,\theta)i(t)} \qquad (2)$$

Arranging the terms we can define the voltage of a phase being:

$$\boldsymbol{v = Ri + l(i,\theta)\frac{di}{dt} + e} \qquad (3)$$

$$\boldsymbol{e = i\omega\frac{dl(i,\theta)}{d\theta}} \qquad (4)$$

$$\boldsymbol{\omega = \frac{d(\theta)}{dt}} \qquad (5)$$

$$\boldsymbol{T_e = i^2\frac{1}{2}\frac{dl(\theta)}{d\theta}} \qquad (6)$$

$$T_m = T_e - D\omega - J\frac{d\omega}{dt} \qquad (7)$$

Where $\boldsymbol{T_m}$ is the mechanical torque, $\boldsymbol{T_e}$ is the electromagnetic torque, ω is the angular velocity, $\boldsymbol{J}$ is the moment of inertia and $\boldsymbol{D}$ is the viscous friction coefficient.

Using the equations of electrical and mechanical behavior of the Switched Reluctance Machine acting as motor. Reorganizing the equations and rewriting in the matrix form, equation 8, so that it facilitates the calculations for its solution [11].

$$\begin{bmatrix} v_a \\ v_b \\ v_c \\ v_d \\ T_m \\ 0 \end{bmatrix} = \begin{bmatrix} r_a & 0 & 0 & 0 & 0 & 0 \\ 0 & r_b & 0 & 0 & 0 & 0 \\ 0 & 0 & r_c & 0 & 0 & 0 \\ 0 & 0 & 0 & r_d & 0 & 0 \\ r_1 & r_2 & r_3 & r_4 & -D & 0 \\ 0 & 0 & 0 & 0 & -1 & 0 \end{bmatrix} \begin{bmatrix} i_a \\ i_b \\ i_c \\ i_d \\ \omega \\ \theta \end{bmatrix} +$$

$$\begin{bmatrix} l_a(i,\theta) & 0 & 0 & 0 & 0 & i_a\frac{\partial l_a(i,\theta)}{\partial\theta} \\ 0 & l_b(i,\theta) & 0 & 0 & 0 & i_b\frac{\partial l_b(i,\theta)}{\partial\theta} \\ 0 & 0 & l_c(i,\theta) & 0 & 0 & i_c\frac{\partial l_c(i,\theta)}{\partial\theta} \\ 0 & 0 & 0 & l_d(i,\theta) & 0 & i_d\frac{\partial l_d(i,\theta)}{\partial\theta} \\ 0 & 0 & 0 & 0 & -J & 0 \\ 0 & 0 & 0 & 0 & 0 & 1 \end{bmatrix} \begin{bmatrix} \dot{i}_a \\ \dot{i}_c \\ \dot{i}_c \\ \dot{i}_d \\ \dot{\omega} \\ \dot{\theta} \end{bmatrix} \qquad (8)$$

$$r_1 = \frac{1}{2}.i_a\frac{\partial l_a(i,\theta)}{\partial\theta},\ r_2 = \frac{1}{2}.i_b\frac{\partial l_b(i,\theta)}{\partial\theta},$$

$$r_3 = \frac{1}{2}.i_c\frac{\partial l_c(i,\theta)}{\partial\theta}, r_4 = \frac{1}{2}.i_d\frac{\partial l_d(i,\theta)}{\partial\theta} \qquad (9)$$

where v_a, v_b, v_c and v_d are the phase voltages; r_a, r_b, r_c and r_d are the winding resistances; l_a, l_b, l_c and l_d are the phase inductances and i_a, i_b, i_c and i_d are the phase currents.

This matrix defines the model of an SRM 8x6 operating as a motor. The SRM 6x4 model operating as an motor is similar just by disregarding the effects of one phase of the matrix. Thus, arranging the terms we can write in the form of an equation of states, Equation 10, which allows to obtain the behavior of the machine at any time.

$$[\dot{I}] = [L]^{-1}[V] - [L]^{-1}[R][I] \tag{10}$$

Using the resources available on the MATLAB™/Simulink® platform, we developed the simulations for the proposed application.

4. Simulation of the Switched Reluctance Motor

To perform the computer simulation, the inductance curves of the machines, Fig.4 for 8x6 and Fig.5 for 6x4 were used.

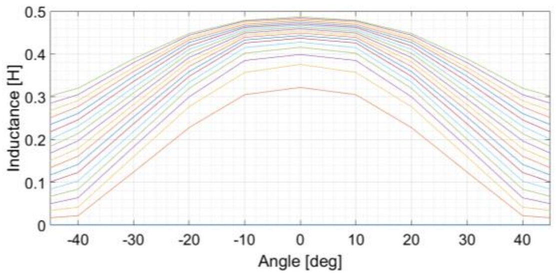

Fig.4. Inductance Curves for SRM 8x6.

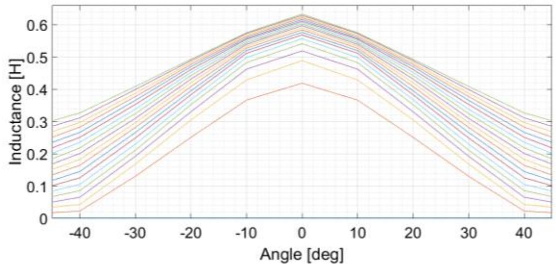

Fig.5. Inductance Curves for SRM 6x4.

The diagram containing the structures for the computational simulation calculation is presented in Fig.6.

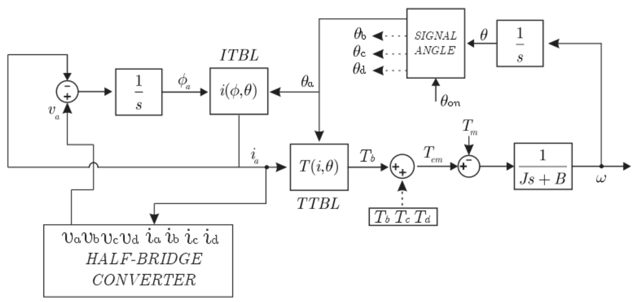

Fig.6. Diagram containing the structures for the computational.

The phase excitation is performed by means of a static converter. It has the function of magnetizing the phase windings independently, exciting the phases according to the rotor relationship with the machine stator.

To start the machines, the Half-bridge (HB) converter was used. The converter is similar for both machines being the SRM 8x6 with 4 phases and the SRM 6x4 with three phases. Fig.7 shows the convert in question for SRM 8x6, SRM 6x4 and similar just by disregarding one phase.

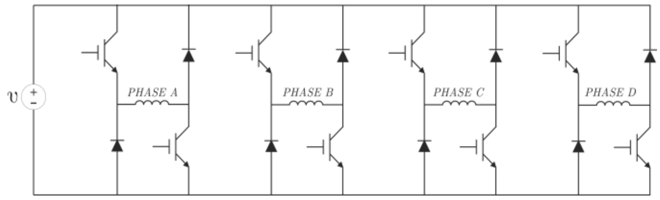

Fig.7. Half-bridge converter.

A. Position sensor

The sensor estimates the stator relation to the machine rotor, comparing them with the user defined conduction angle limits, thus returning the phase activation signal. This signal is generated when the poles are aligning with a phase, showing minimal reluctance or when the phase is misaligned, thus having maximum reluctance. Fig.8 shows the diagram of this sensor.

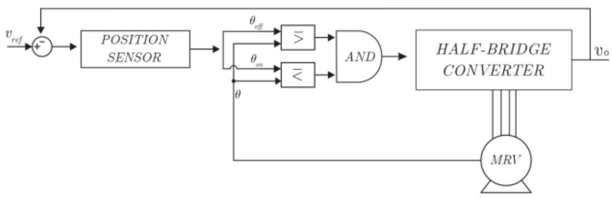

Fig.8. Position sensor diagram.

B. Current control

To ensure safety for machine operation, a current control has been implemented. In this control the user sets a reference current ($\boldsymbol{i_{ref}}$). To perform this control it is necessary to estimate the operating range, which is the error that is the difference between the activation current and the phase current. The current error is passed through the relay block, which determines whether it is above ($\boldsymbol{i_{on}}$) or below ($\boldsymbol{i_{off}}$) the desired limit around the reference current input error. Then the signal is sent to the converter, which magnetizes the phases if the current is between the operating limits. The waveform with this control is represented in Fig.9.

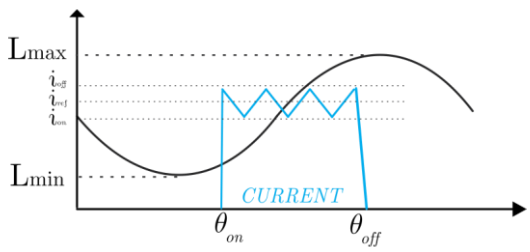

Fig.9. Signal shape with current control actuation.

To optimize the machine performance, current control was used in only one of the coils of each phase, the others being driven directly by the position sensor signal. The diagram of this block is shown in Fig.10.

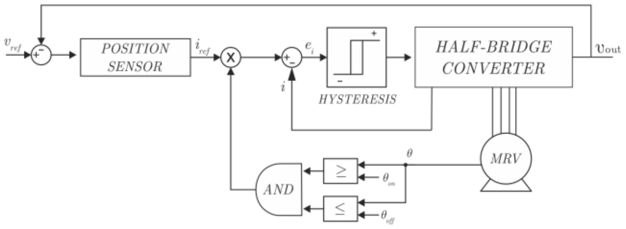

Fig.10. Current Controller Diagram.

C. Speed control

To control the speed of the SRM was used the proportional and integral controller (PI), which causes the system to reach the reference speed specified by the operator. The control acts on the power of the machine causing the speed to change depending on the excitation of the machine. Fig.11 shows the system loop diagram with the PI control.

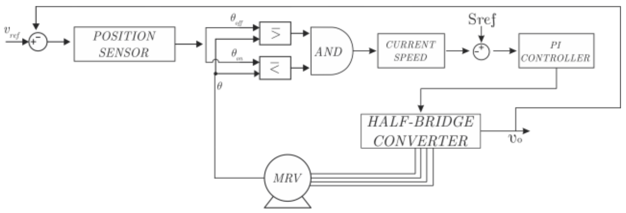

Fig.11. PI controller diagram for speed.

D. Efficiency

To estimate the performance of the SRM a block was developed to calculate the efficiency (η) of each machine, represented by equation 11, where the input power is calculated by the product of the converter current and supply voltage, already output power is the product of motor speed with torque.

$$\eta = \frac{T_e * \omega_r}{v * i} \quad (11)$$

E. Switching System

The most common SRM drive is the system known as single pulse drive. In this system, during inductance growth, both switches of the HB converter. receive at their control terminals a pulse to allow the phase coil to magnetize or demagnetize. The need to control some quantities such as current speed, and SRM conjugate requires that some switching techniques be employed to perform the control. To avoid the machine is to perform the control and it is necessary to switch keys, and this ends up generating losses in the process. Therefore it is necessary to look for techniques that minimize switching losses.

Thus, the soft chopping switching system was employed, in which the lower switch of the HB converter is kept constant during the driving angle, while the upper switch of the converter is switching according to the required control need. The system can be observed in the Fig.12.

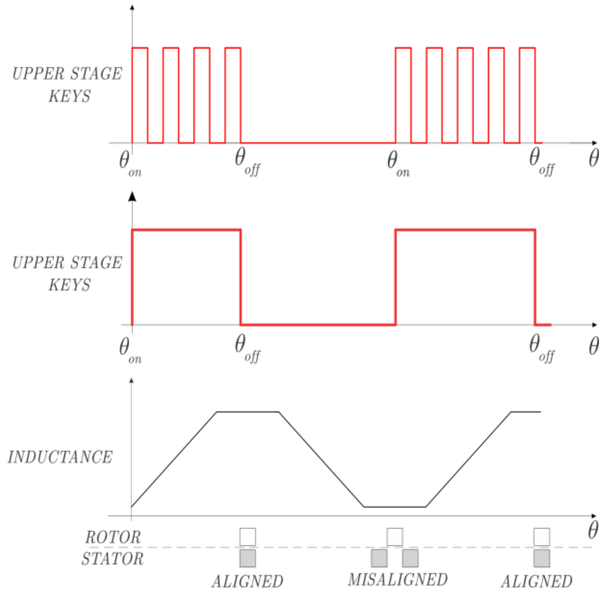

Fig.12. Switching system waveforms.

In general, this method presents lower levels of acoustic noise and electromagnetic interference. Such a switching strategy also has lower ripple levels in the current and affects the performance of the machine [12][13].

5. Simulation Results

Next, we will show several curves that validate the experimental simulation. Initially, Fig.13 shows the action of the PI control on two machines with equal operating conditions, where the speed setpoint remains constant at 500rpm until 0.3 seconds, and the setpoint is changed to 2000 rpm and remains at this speed. Speed up to 0.6 seconds in sequence and set the speed to 1600 rpm and keep it that way.

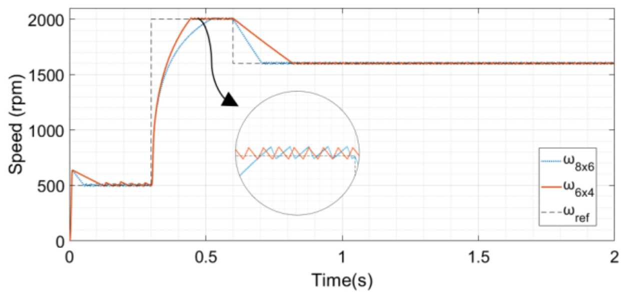

Fig.13. SRM speed with PI controller actuation.

The performance of the machines is shown in Fig.14. The curves were plotted with the same operating conditions used for speed control.

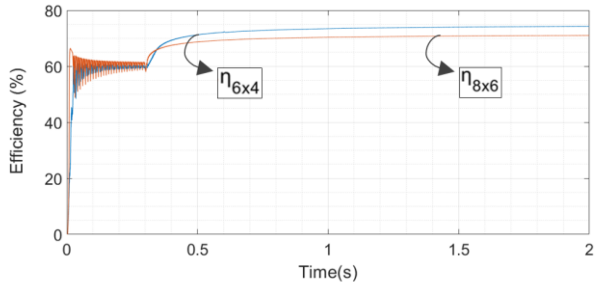

Fig.14. SRM efficiency.

The Fig. 15, represents the efficiency of the SRM 8x6 applied to the new drive system, it is possible to verify that using the soft chopping system there was an increase in its yield, caused by the reduction of losses in the system.

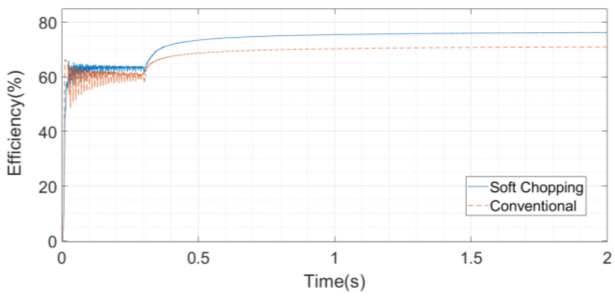

Fig.15. SRM 8x6 efficiency with soft chopping

4. Conclusion

This paper presents a comparative study between two 60 kW SRM, one of them is a three-phase 6x4 pole machine and the other an 8x6 four-phase machine.

The computer simulation was modeled from the magnetization curves of the machines. Graphs were generated using current and speed control.

Analyzing the results obtained through the computer simulation it was verified that the SRM 8x6, presents less oscillation in the conjugate than the SRM 6x4, under the same operating conditions. In addition, it was found that SRM 8x6 has lower performance than SRM 6x4.

Acknowledgement

The authors would like to thank Federal Institute of Education, Science and Technology Goiás - Campus of Itumbiara for the contribution

References

[1] MORAIS, Luciano Cardoso de. Study on the panorama of electric energy in Brazil and future trends. 2015. 127 p. Dissertation (masters) - Paulista State University Julio de Mesquita Filho, Faculty of Engineering, 2015.

[2] SILVEIRA, Augusto Wohlgemuth Fleury Veloso da. On-load voltage control for motor / generator at three phase variable reluctance. 2012. 202 f. Thesis (Doctorate in Engineering) - Federal University of Uberlândia, Uberlândia, 2012.

[3] N. Radimov, N. Ben-Hail and R. Rabinovici, "Simple model of switched-reluctance Machine based only on aligned and unaligned position data," in IEEE Transactions on Magnetics, vol. 40, no. 3, pp. 1562-1572, May 2004.

[4] ICHINOKURA, Osamu & Kikuchi, Tsukasa & Nakamura, Kenji & Watanabe, Tadaaki & Guo, Hai-Jiao. (2003). Dynamic Simulation Model of Switched Reluctance Generator. Magnetics, IEEE Transactions on. 39. 3253 - 3255.

[5] RILEY, Chris P. et al. Simulation based design of reluctance motors for traction applications in hybrid and electric vehicles. In: 7th IET International Conference on Power Electronics, Machines and Drives (PEMD 2014). EIT, 2014. p. 1-6.

[6] BOBER, Peter. Measurement of Objective Function for BLDC Motor Optimization. Acta Electrotechnica et Informatica, v. 17, no. 4, p. 43-49, 2017 ..

[7] PTAKH, G. K. Switched reluctance drive medium and high power: foreign and domestic experience. Russian Internet Journal of Electrical Engineering, v. 2, no. 3, p. 23-33, 2016 ..

[8] L. Kolomeitsev et al., "Linear switched reluctance engine as a high efficiency propulsion system for railway vehicles," 2008 International Symposium on Power Electronics, Electrical Drives, Automation and Motion, Ischia, 2008, pp. 155-160.

[9] Hu, Yihua et al. Modular tri-port high-power converter for SRM based plug-in hybrid electrical trucks. IEEE Transactions on Power Electronics, v. 33, no. 4, p. 3247-3257, 2017 ..

[10] Krishnan, R. (2001). Switched Reluctance Motor Drives: Modeling, Simulation, Analysis, Design, and Applications. Systems & Control Letters - SYST CONTROL LETT.

[11] SILVEIRA, Augusto Wohlgemuth Fleury Veloso da. On-load voltage control for motor / generator at three phase variable reluctance. 2012. 202 f. Thesis (Doctorate in Engineering) - Federal University of Uberlândia, Uberlândia, 2012.

[12] GAN, Chun et al. Low-cost direct instantaneous torque control for switched reluctance motors with bus current detection under soft-chopping mode. EIT Power Electronics, v. 9, no. 3, p. 482-490, 2016.

[13] Mollet, Yves et al. Experimental noise and vibration analysis of switched reluctance machines comparison of soft and hard chopping in transient conditions. In: 2015 International Conference on Renewable Energy Research and Applications (ICRERA). IEEE, 2015. p. 420-425.